J. Biochem. 126, 545-552 (1999)

# β-Glycosidase from the Hyperthermophilic Archaeon *Sulfolobus solfataricus*: Structure and Activity in the Presence of Alcohols[1]

**Sabato D'Auria,*[,2] Roberto Nucci,* Mose' Rossi,* Enrico Bertoli,† Fabio Tanfani,† Ignacy Gryczynski,‡ Henry Malak,‡ and Joseph R. Lakowicz‡**

*Istituto di Biochimica delle Proteine ed Enzimologia, C.N.R., Via Marconi, 10 80125 Naples, Italy; †Istituto di Biochimica, Facolta' di Medicina e Chirurgia, Universita' di Ancona, Italy; and ‡University of Maryland, School of Medicine, Baltimore, Maryland 21201, USA

Received May 20, 1999; accepted June 30, 1999

**β-Glycosidase from the extreme thermophilic archaeon *Sulfolobus solfataricus* is a tetrameric protein with a molecular mass of 240 kDa, stable in the presence of detergents, and with a maximal activity at temperatures above 95°C. Understanding the structure-activity relationships of the enzyme under different conditions is of fundamental importance for both theoretical and applicative purposes. In this paper we report the effect of methanol, ethanol, 1-propanol, and 1-butanol on the activity of *S. solfataricus* β-glycosidase expressed in *Escherichia coli*. The alcohols stimulated the enzyme activity, with 1-butanol producing its maximum effect at a lower concentration than the other alcohols. The structure of the enzyme was studied in the presence of 1-butanol by circular dichroism, and Fourier-transform infrared and fluorescence spectroscopies. Circular dichroism and steady-state fluorescence measurements revealed that at low temperatures the presence of the alcohol produced no significant changes in the tertiary structure of the enzyme. However, time-resolved fluorescence data showed that the alcohol modifies the protein microenvironment, leading to a more flexible enzyme structure, which is probably responsible for the enhanced enzymatic activity.**

**Key words: archaeon, circular dichroism, frequency domain fluorometry, β-glycosidase, infrared spectroscopy, organic solvent.**

Enzymes isolated from hyperthermophilic micro-organisms are not only thermostable and active at high temperature, but are also often resistant to and active in the presence of organic solvents and detergents (*1, 2*). In the presence of common denaturants, such enzymes generally show increased stability compared with their mesophilic counterparts. These proteins represent natural examples of proteins with very peculiar and interesting properties (*3, 4*). The goal of many studies is to identify the molecular basis of their stability and use them as models for designing proteins with special properties for new biotechnological applications (*5, 6*). However, how the effect of organic solvents is related to the most unusual properties of thermophilic enzymes, such as the thermostability and thermoactivity, remains unanswered.

A thermophilic and thermostable β-galactosidase from the archaeon *Sulfolobus solfataricus* (*7*) has been purified and partially characterized in our laboratories (*8*). More recently, the enzyme was characterized as a glycosyl hydrolase, and, in view of its wide substrate specificity and exo-glucosidase activity, it has been classified as a β-glycosidase (Sβgly) (*9*). Its gene has been cloned and expressed both in *Escherichia coli* (*10*) and *Saccharomyces cerevisiae* (*11*). The recombinant enzymes were purified, and shown to have the same structural and functional features of the native enzyme (*12, 13*). The native and recombinant enzymes have a molecular mass of about 240 kDa, and are composed of four identical subunits of about 60 kDa, each of which contains 17 tryptophan residues. Moreover, the native enzyme has been crystallized (*14*) and its structure solved at 2.6 Å (*15*). The crystallographic data show that the enzyme contains more than double the proportion of ionic groups involved in ion pairs than is generally present in mesophilic proteins (*16*), and that these pairs are involved in clusters and networks that serve to cross-link non-contiguous points of the structure at the protein surface.

In some recent papers (*17-23*) we have shown the effect of temperature, sodium dodecyl sulfate, and basic pH conditions on the structure, activity, and conformational dynamics of the enzyme. In the present study we have

[1] This work was supported by a grant from the Ministry for University and for Technological and Scientific Research (M.U.R.S.T.) "Programma Nazionale Biocatalisi e Bioconversioni" (E.B., F.T.), an EU contract "Extremophiles" (M.R., S.D., R.N.), and by the National Center for Research Resources, NIH RR-08119 (J.R.L., I.G., H.M.).
[2] To whom correspondence should be addressed at: University of Maryland at Baltimore, School of Medicine, Center for Fluorescence Spectroscopy, 725 W Lombard Street 21201 Baltimore MD, USA. Phone: +1-410-706-7500, Fax: +1-410-706-8408, E-mail: dauria@dafne.ibpe.na.cnr.it

Abbreviations: Sβgly, *Sulfolobus solfataricus* β-glycosidase; CD, circular dichroism; FT-IR, Fourier-transform infrared spectroscopy; ONPG, *o*-nitrophenyl-β-D-galactopyranoside; amide I′, amide I band in $D_2O$ medium.

investigated the effects of a series of aliphatic alcohols on the structure and activity of Sβgly by far-, near-UV circular dichroism (CD), Fourier transform infrared spectroscopy (FT-IR), and steady-state fluorescence spectroscopy. The conformational dynamics of the enzyme were studied by frequency domain fluorometry and anisotropy decays.

## EXPERIMENTAL PROCEDURES

*Reagents*—$NaH_2PO_4 \cdot H_2O$ was obtained from J.T. Baker Chemicals (New York, NY, USA). Deuterium oxide (99.9% $^2H_2O$) and $CH_3(CH_2)_3OD$ were purchased from Aldrich. All other chemicals were commercial samples of the purest quality. Deuterated 1-butanol is reported throughout the paper as 1-butanol.

*Enzyme Purification and Assay*—The procedure for the preparation of homogeneous Sβgly is described elsewhere (*9*). Protein samples were concentrated and placed in 10 mM sodium phosphate buffer, pH 7.4, with an Amicon ultrafiltration apparatus using PM-30 membranes.

Enzyme activity was measured by following the hydrolysis of *o*-nitrophenyl-β-D-galactopyranoside (ONPG) in the absence and presence of the specified amounts of alcohol from 30-75°C in sealed quartz cuvettes as previously described (*9*). Each enzyme activity value is the mean of at least three independent determinations. Standard deviations never exceeded 10% of the respective mean values.

*Protein Assay*—Protein concentration was determined by the method of Bradford (*24*), with bovine serum albumin as the standard, and by $A_{280}$ in 50 mm sodium phosphate buffer, pH 7.0, at 25°C in a double beam Cary 1E spectrophotomer (Varian, Mulgrade, Victoria, Australia) giving a value of $6.95 \times 10^5$ absorbance units/mol (*13*).

*Circular Dichroism Spectroscopy*—Circular dichroism spectroscopy (CD) was performed on homogeneous samples of Sβgly at concentrations between 0.2 and 0.5 mg/ml in 10 mM sodium phosphate buffer, pH 7.4, plus the specified amounts of alcohol. We used a J-710 spectropolarimeter (Jasco, Tokyo) equipped with a Neslab RTE-110 temperature-controlled liquid system (Neslab Instruments, Portsmouth, NH, USA) calibrated with a standard solution of (+)-10-camphorsulfonic acid. Sealed cuvettes with 0.1 and 1.0 cm path lengths (Helma, Jamaica, NJ, USA) were used for the far- and near-UV regions, respectively. Photomultiplier voltage did not exceed 600 V in the spectral regions measured. Each spectrum was averaged five times and smoothed with Spectropolarimeter System Software version 1.00 (Jasco). All measurements were performed under nitrogen flow. For CD analyses, all samples were preincubated for 10 min at the temperature being studied. The results are expressed in terms of molar ellipticity ($\theta$).

*Preparation of Samples for Infrared Measurements*—Typically, 1.0 mg of Sβgly in 1.0 ml of buffer was centrifuged in a "30 K microsep" microconcentrator (Dasit) at $3,000 \times g$ and 4 C to a volume of approximately 50 μl. Then 300 μl of buffer A (50 mM Hepes pD 7.4) or buffer B (50 mM Hepes, 300 mM 1-butanol pD 7.4) or buffer C (50 mM Hepes, 80 mM 1-butanol pD 7.4) were added and the sample was concentrated again. This procedure was repeated several times in order to completely replace the original buffer with A or B or C buffers. In the last washing all samples were concentrated to a final volume of approximately 40 μl and used for infrared analyses.

*Infrared Spectra*—The concentrated protein samples in the final buffers were placed in a thermostated Graseby Specac 20500 cell (Graseby Specac, Orpington, Kent, UK) fitted with $CaF_2$ windows and 25 μm spacers. FT-IR spectra were recorded by means of a Perkin-Elmer 1760-× Fourier transform infrared spectrometer using a deuterated triglycine sulfate detector and a normal Beer-Norton apodization function. For at least 24 h before, and during data acquisition the spectrometer was continuously purged with dry air at a dew point of −40°C. Spectra of buffers and samples were acquired at 2 $cm^{-1}$ resolution under the same scanning and temperature conditions. In the thermal-denaturation experiments, the temperature was raised in 5°C steps from 20 to 95°C. Before spectrum acquisition, samples were maintained at the desired temperature for the time necessary to stabilize the temperature inside the cell (6 min). Second derivative spectra were calculated over a 9 data-point range (9 $cm^{-1}$). The deconvolution parameters for the amide I′ band were set with the half-bandwidth at 17 $cm^{-1}$ and a resolution enhancement factor of 2.125.

*Fluorescence Spectroscopy*—Emission spectra were obtained with a Jasco FP777 spectrofluorimeter, at a protein concentration of 0.05 mg/ml in 10 mM sodium phosphate buffer, pH 7.4, plus the specified amounts of alcohol. The excitation was set at 300 nm in order to exclude the tyrosine contribution to the overall fluorescence emission.

Frequency domain data were obtained with a frequency domain fluorimeter operating between 2 and 2,000 MHz (*25-27*). Modulated excitation was provided by the harmonic content of a laser pulse train with a repetition rate of 3.75 MHz and a pulse width of 5 ps, from a synchronously pumped and cavity dumped rhodamine 6G dye laser. The dye laser was pumped with a mode-locked argon ion laser (Coherent, Innova 100). The dye laser output was frequency doubled to 300 nm for tryptophan excitation. For intensity decay measurements, magic angle polarizer orientations were used. The emitted light was observed through an interference filter at 340 nm. The frequency-domain intensity data were fitted to the time-resolved expression

$$I(t) = \sum_i \alpha_i e^{-t/\tau_i}$$

where $\alpha_i$ are the pre-exponential factors, $t$, the decay times, and $\Sigma\alpha_i = 1.0$. The frequency-domain anisotropy data were fitted to

$$\gamma(t) = \sum_i \gamma_i e^{-t/\theta_i}$$

where $r_i$ are the amplitudes with rotational correlation times $\theta_i$. The parameters were recovered by nonlinear least squares using the theory and software described elsewhere (*28, 29*). The standard deviations for phase and modulation were 0.3 and 0.005, respectively.

## RESULTS AND DISCUSSION

SβGly is one of the more extensively studied thermophilic enzymes (*15, 17-23*). Structure resolution at 2.6 Å shows the enzyme to be a tetramer with each subunit having the classic $(\beta\alpha)_8$-fold and lying at the corner of a slightly puckered square in contact with two other monomers. Of the 524 charged groups in the protein, 58% are involved in

ion-pair interactions, and about 60% of them occur as a part of multiple ion pair networks with at least three charged centers (*15*). These findings, according to other reports (*19-20, 22-23*), suggest that large ion-pair networks play a key role in the structural organization and thermostability of the protein. Moreover, Sβgly contains 68 tryptophan residues (17 residues per subunit) that are homogeneously dispersed in the primary structure and organized in clusters in the tertiary structure (*15*). These features make Sβgly an attractive model for studies of the structure-function relationship of proteins.

*Enzyme Activity in the Presence of Alcohols*—The effects of methanol, ethanol, 1-propanol, and 1-butanol on the activity of Sβgly were studied at 30°C and the results are shown in Fig. 1. In all instances, enzyme activation was observed depending on the concentration of the alcohol as well as its alkyl chain length. The alcohol concentration at which the maximal Sβgly activity was observed decreased with increasing length of the alcohol chain: maximal activation was induced by 80 mM 1-butanol (130%). Moreover, the activation observed at 30°C became less with increasing temperature and at 75°C was only 10%. Table I shows the kinetic parameters of Sβgly in the absence and in the presence of 80 mM 1-butanol at 30 and 75°C. At 30°C, Sβgly in the presence of 1-butanol shows a $K_m$ value of 0.5 mM, which is twofold lower than that shown in the absence of the alcohol, suggesting that the presence of 1-butanol increases the enzyme affinity for substrate. The catalytic efficiency values of Sβgly in the presence and absence of 80 mM 1-butanol (110 *versus* 24 $s^{-1}$/mM) suggest that at 30°C the enzyme is 4.58-fold more efficient in the presence of the alcohol. However, at 75°C, Sβgly shows a $K_m$ value of 11.0 mM in the presence of 80 mM 1-butanol as compared to 4.0 mM in its absence, and the catalytic efficiency is only 40% of that detected at the same temperature in the absence of the alcohol. These data suggest that at high temperature 1-butanol affects enzyme stability.

In order to investigate the effect of 1-butanol on the structural features of Sβgly we characterized the enzyme by CD and FT-IR. We selected two 1-butanol concentrations, 80 mM, the concentration that induces the maximal enzyme activation, and 300 mM, which affects the enzyme activity (Fig. 1).

*Circular Dichroism*—The circular dichroism (CD) spectrum for Sβgly in the far-ultraviolet region pH 7.4 and 30°C shows two minima, at 208 and 222 nm. Analysis of the CD data provided the following information about the secondary structure: α-helices, 50%; β structures, 40%; turns, 10%; unordered structures, less than 1% (*17*). Moreover, the far-UV CD spectra recorded in the temperature range 20-95°C were superimposable suggesting that the secondary structural organization of the thermohilic enzyme is unaffected by temperature. The addition of 1-butanol at concentrations of 80 or 300 mM to the enzyme solution at 20°C did not modify the CD spectrum; moreover, Sβgly in the presence of 80 or 300 mM 1-butanol displayed the same CD spectra at 25 and 85°C (data not shown).

The near-UV CD spectrum of Sβgly in the absence of 1-butanol at 30°C (Fig. 2) suggests that most of the aromatic residues in the protein are constrained by tertiary interactions in compact regions of the protein macromolecule. The minimum at 293 and the maxima at 274 and 260 nm can be ascribed to tryptophan, tyrosine, and phenylalanine residues, respectively (*30*). The addition of 80 or 300 mM 1-butanol to the enzyme solution resulted in only a slight effect on the side chains of Sβgly up to a temperature of 70°C. However, starting from 75°C, the

TABLE I. **Kinetic parameters of Sβgly in the absence and presence of 80 mM 1-butanol.**

| Temperature (°C) | Absence | | | Presence | | |
|---|---|---|---|---|---|---|
| | $K_m$ (mM) | $k_{cat}$ ($s^{-1}$) | $k_{cat}/K_m$ ($s^{-1}$/mM) | $K_m$ (mM) | $k_{cat}$ ($s^{-1}$) | $k_{cat}/K_m$ ($s^{-1}$/mM) |
| 30 | 1.0 | 24 | 24 | 0.5 | 55 | 110 |
| 75 | 4.0 | 1,320 | 330 | 11.0 | 1,450 | 131.88 |

The kinetic parameters were determined using *o*-nph-β-D-Galp as a substrate in the absence and presence of 80 mM 1-butanol.

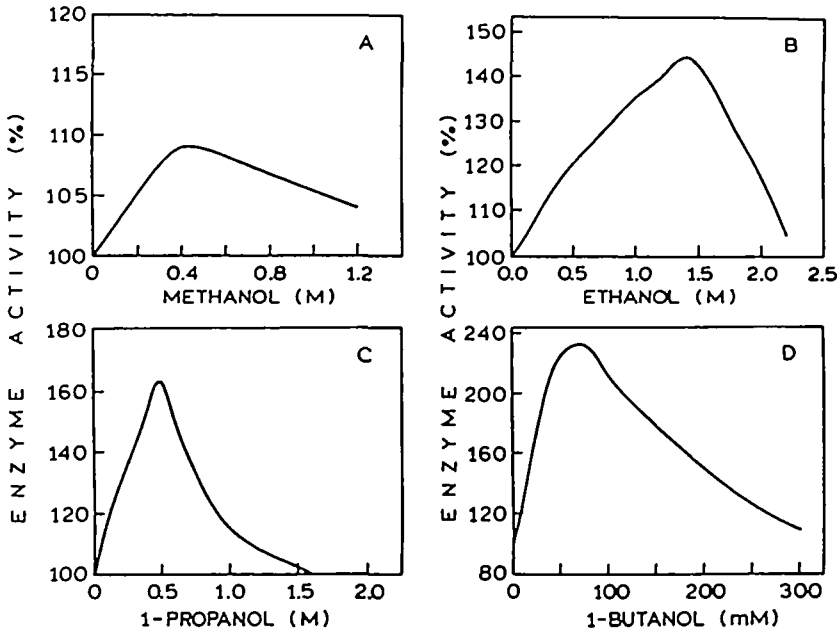


Fig. 1. **Enzymatic activity of Sβgly at 30°C in the presence of methanol (A), ethanol (B), 1-propanol (C), and 1-butanol (D).**

enzyme displayed marked changes in the CD spectrum in the presence of 80 mM or 300 mM 1-butanol, and at 85°C a strong quenching of the dichroic activity was observed, indicating that the stability of the protein is affected by the presence of alcohol at high temperature (Fig. 2). In contrast, S$\beta$gly in the absence of 1-butanol displayed the same near-UV CD spectra in the temperature range 25-95°C, indicating that the tertiary architecture of the protein is not affected by high temperature (*17*).

*Infrared Spectroscopy*—In a previous paper (*20*), we described the structure of S$\beta$gly at basic pH and in the presence of SDS. Figure 3 shows the second derivative and deconvolved spectra of S$\beta$gly at pD 7.4 and 10. The spectra are similar in shape, but differences in band positions and intensities are present indicating differences in the secondary structure of the enzyme at the two different pDs. In particular, at pD 7.4, the band related to $\beta$-sheets (*20*) is found at a higher wavenumber (1,636.6 $cm^{-1}$) than at pD 10 (1,635.1 $cm^{-1}$), suggesting that at pD 7.4 the $\beta$-sheets are less exposed to the solvent. The intensity of the residual amide II band (1,548 $cm^{-1}$) at pD 7.4 is higher than at pD 10, also suggesting that at pD 7.4 the protein is less accessible to the solvent ($D_2O$) than at pD 10. At pD 7.4, a unique 1,682.8 $cm^{-1}$ band is found, which is probably due to turns and $\beta$-sheets since at pD 10 the band splits into two bands, which were previously assigned to turns and $\beta$-sheets (*20*). The bands at 1,667.2, 1,654.9, and 1,645 $cm^{-1}$ are assigned to turns, $\alpha$-helices, and unordered structures, respectively (*20*). The other bands seen in the 1,600-1,500 $cm^{-1}$ region and not already mentioned can be assigned to amino acid side chain absorptions (*31*). The presence of 300 mM 1-butanol affects the secondary structure of S$\beta$gly at pD 7.4 only marginally as revealed by the second derivative and deconvolved spectra of the enzyme (data not shown). The residual amide II band intensities of S$\beta$gly in the absence and presence of 300 mM 1-butanol are similar, indicating that the accessibility of the solvent ($D_2O$) to the protein is similar for both samples. The small differences between the spectra of S$\beta$gly in the absence and presence of 300 mM 1-butanol appear even smaller when comparing the spectra of the control with the spectra of S$\beta$gly in the presence of 80 mM 1-butanol (data not shown).

*Thermal Denaturation of S$\beta$gly*—The thermal denaturation of S$\beta$gly was followed by monitoring different parameters of the infrared spectra. Figure 4 shows the amide I′ bandwidth as a function of temperature (*32*), and Fig. 5 shows difference spectra from which detailed information about protein denaturation and aggregation can be obtained (*33*). The spectra shown in Fig. 5 are the difference between the two original absorption spectra collected at close temperatures as indicated in the figure. The broad negative band in the amide I′ region reflects thermal denaturation (loss of secondary structure) while the positive bands close to 1,617 and 1,685 $cm^{-1}$ are due to protein aggregation brought on by thermal denaturation (*33*). Figure 5A shows

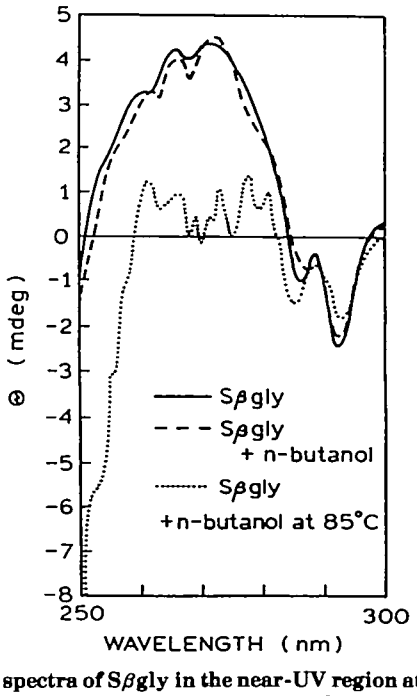


**Fig. 2. CD spectra of S$\beta$gly in the near-UV region at 30°C in the absence (continuous line) and presence of 1-butanol (dashed line), and at 85°C in the presence of 1-butanol (dotted line).**

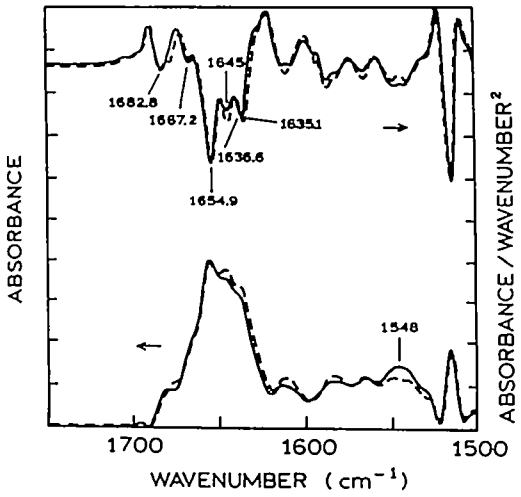


**Fig. 3. Second derivative (top) and deconvolved (bottom) spectra of S$\beta$gly.** Continuous and dashed lines refer to S$\beta$gly spectra at pD 7.4 and 10.1, respectively.

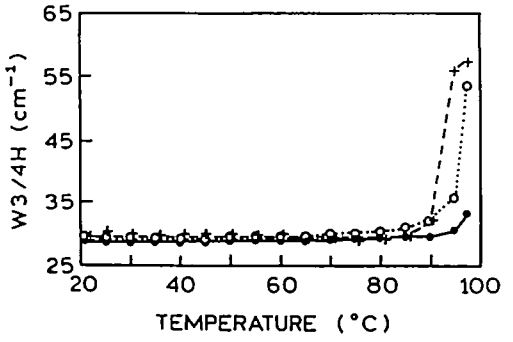


**Fig. 4. Thermal denaturation of S$\beta$gly in the absence and presence of 1-butanol (300 mM).** The amide I′ width calculated as 3/4 of amide I′ eight (W3/4H) was monitored as a function of temperature. Continuous line and closed circles: S$\beta$gly in the absence of 1-butanol at pD 7.4; dotted line and open circles: S$\beta$gly in the presence of 1-butanol at pD 7.4; dashed line and crosses: S$\beta$gly in the absence of 1-butanol at pD 10.1.

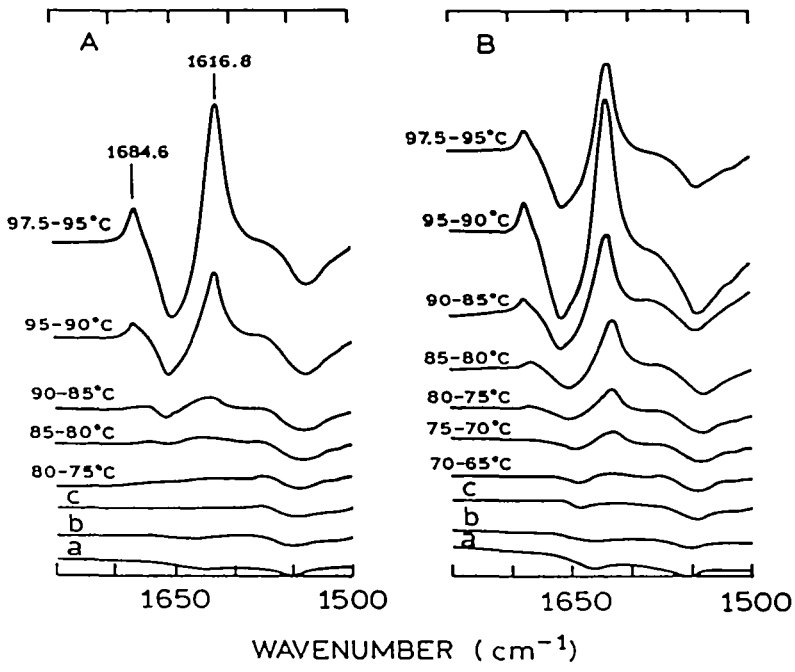


Fig. 5. **Difference spectra of Sβgly in the absence (panel A) and presence (panel B) of 1-butanol (300 mM) at pD 7.4.** Difference spectra are the difference between two original absorbance spectra recorded at close temperatures as indicated on the figure (*e.g.* 95-90°C). Spectra a, b, and c represent difference spectra 25-20, 45-40, and 65-60°C, respectively.

that at pD 7.4 protein denaturation and aggregation occur concomitantly and to a large extent between 95 and 97.5°C. However, Fig. 4 shows that at these temperatures protein denaturation has just started (or is not complete). In the presence of 300 mM 1-butanol (Fig. 5B), the maximal denaturation and aggregation of Sβgly occurs apparently between 90 and 95°C, as shown by the high intensities of the negative and positive peaks. However, it must be noted that the difference spectrum obtained at these temperatures should be divided by 2 in order to be compared with the difference spectrum (97.5-95°C) in which the temperature increment is 2.5°C. Taking this into account, the maximal denaturation and aggregation of the protein occurs between 95 and 97.5°C as shown also by the thermal denaturation curve shown in Fig. 5. The onset of denaturation and aggregation of Sβgly can be observed between 85 and 90°C and 75 and 80°C in the absence and presence of 1-butanol, respectively (Fig. 4). These spectra indicate that 300 mM 1-butanol decreases the protein stability as shown also by the thermal denaturation curves shown in Fig. 4, although in this figure the identification of the onset of denaturation is less certain than in the difference spectra. Figure 4 also shows the thermal denaturation of Sβgly at pD 10. The high pD destabilizes the protein structure to a larger extent than 1-butanol since the maximal denaturation is observed between 90 and 95°C at pD 10 and between 95 and 97.5 °C in the presence of alcohol at pD 7.4. The negative band close to 1,545 $cm^{-1}$ in the difference spectra is due to a further H/D exchange that occurs at high temperatures as a consequence of the loosening of the protein structure and/or protein denaturation, both allowing the solvent ($D_2O$) to reach more protein segments.

The thermal denaturation curves and the difference spectra of Sβgly in the presence of 80 mM 1-butanol were very similar to those of the control (data not shown), indicating the same secondary structure stability in both samples. However, it is interesting to note that CD revealed a destabilization of the Sβgly tertiary structure at 85°C, a phenomenon that could not be observed by infrared spectroscopy.

The data presented have indicated that both pH and solvent affect the structure and activity of Sβgly. At pD 7.4 the structure of the protein is less accessible to solvent than at pD 10, as indicated both by the positions of the β-sheet band and by the intensity of the residual amide II band. These data suggest that the structure of the protein at pD 7.4 is more compact than at pD 10. Moreover, the fact that at pD 7.4 the β-sheet band is found at 1,636.6 $cm^{-1}$ while at pD 10 its position is at 1,635.1 $cm^{-1}$ suggests that at pD 7.4 the β-sheets are more buried in the protein core than at pD 10. In the presence of 1-butanol the positions of the β-sheet and α-helix bands and the residual amide II band intensity are the same as in the control spectrum, indicating that the alcohol does not influence the accessibility of the solvent to the protein. An explanation for this finding could be that 1-butanol might replace some hydrophobic interactions between amino acid residues, probably located near the surface rather than in the protein core. These new hydrophobic interactions would not influence the accessibility of the solvent to the protein surface but would have the effect of destabilizing the structure of the protein to some extent as shown by the thermal denaturation curves. On the other hand, the higher destabilization of the protein structure and the higher accessibility of the solvent to the protein induced by high pHs with respect to 1-butanol indicate that ionic interactions play an important role in the stability of the protein.

*Fluorescence Spectroscopy*—Since CD and FT-IR measurements did not show any relevant effect of 1-butanol on the structure of Sβgly, we performed fluorescence characterization of the enzyme in the absence and presence of 80 mM and 40 mM 1-butanol. These alcohol concentrations, as shown in Fig. 1, induce maximal and 50% maximal enzyme activation, respectively.

The steady-state fluorescence spectra of S$\beta$gly are similar in both the absence and presence of 40 and 80 mM 1-butanol. The fluorescence emission maximum is centered at 339 nm and is blue-shifted compared with the emission maximum of *N*-acetyltryptophanylamide (NATA) (*34*). The quantum yields in the absence and presence of 1-butanol are also the same and close to that observed for NATA under the same experimental conditions.

The intensity and anisotropy decays of the intrinsic fluorescence of S$\beta$gly were measured using the frequency-domain method, and the data were analyzed using mutli-exponential models. Table II shows the multi-exponential analysis of the intensity and anisotropy decays of S$\beta$gly at 30°C in the absence and presence of 40 and 80 mM 1-butanol. The best fits were obtained using the three exponential model, characterized by chi-square values that were much lower than those obtained with the other fits. The mean lifetimes of S$\beta$gly in the absence and in the presence of 40 and 80 mM 1-butanol are 5.74, 5.76, and 5.75 ns, respectively. The steady-state fluorescence data and the mean lifetime of the enzyme in the absence and presence of the alcohol are similar. However, as can be seen in Table II, the addition of the alcohol to the protein solution changed its intensity decay and amplitude values, indicating a solvent effect on the protein microenvironment. S$\beta$gly in the absence of 1-butanol displayed three lifetime components centered at 0.73 ns ($\tau_1$), 3.14 ns ($\tau_2$) and 8.22 ns ($\tau_3$). The middle-lived component ($\tau_2$) is coincides closely with the typical lifetime value observed for monomeric tryptophanyl residues (*34*), while the long-lived component ($\tau_3$) can be ascribed to tryptophan residues located in the compact homogeneous, partly buried, and/or unrelaxed interior of the protein matrix (*34*). The addition of 40 mM 1-butanol to the protein solution resulted in a decrease in the middle- and long-lived components to 2.43 and 8.05 ns, respectively. On the other hand, the short-lived component ($\tau_1$) increased to 1.46 ns. The addition of 80 mM 1-butanol to the enzyme solution caused a decrease in the long-lived component to 7.72 ns, while the middle-lived component remained almost unchanged.

In an attempt to visualize the conformational dynamics of S$\beta$gly alone and in the presence of 40 and 80 mM 1-butanol, we analyzed the data using a lifetime distribution model (*35*). The best fits were obtained from a bimodal distribution with Lorentian shape. Figure 6 shows the S$\beta$gly lifetime distributions in the absence (continuous line) and presence of 80 mM 1-butanol (dashed line), the alcohol concentration that induces the maximal enzyme activation (see Fig. 1). In the absence of the alcohol, two components appear in the lifetime distribution: one with a center at 0.54 ns and the other centered at 2.5 ns. The short component (0.54 ns) is moderately sharp, with a width of 0.6 ns. The long component (2.5 ns) is very broad, 5.9 ns. When 1-butanol was added to the enzyme solution, a quite different S$\beta$gly lifetime distribution was observed (Fig. 6, dashed line). The lifetimes appear separated into two distinct peaks, suggesting that the emissive properties of S$\beta$gly arise from two tryptophan classes, one exposed to the solvent and the other localized in buried and/or unrelaxed regions of the protein matrix. Moreover, the peaks are very sharp suggesting that the addition of the alcohol to the protein solution induces an increase in protein flexibility. In

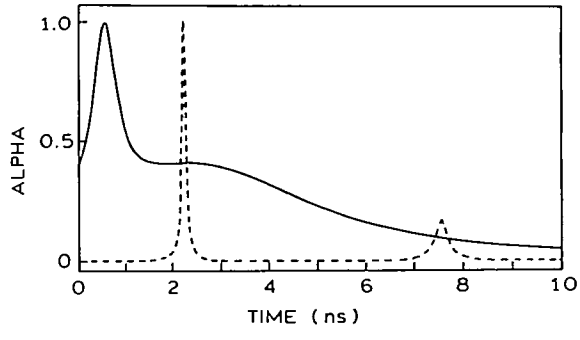


Fig. 6. **Tryptophanyl lifetime distribution pattern of S$\beta$gly in the absence (continuous line) and presence of 80 mM 1-butanol (dashed line) at 30°C.**

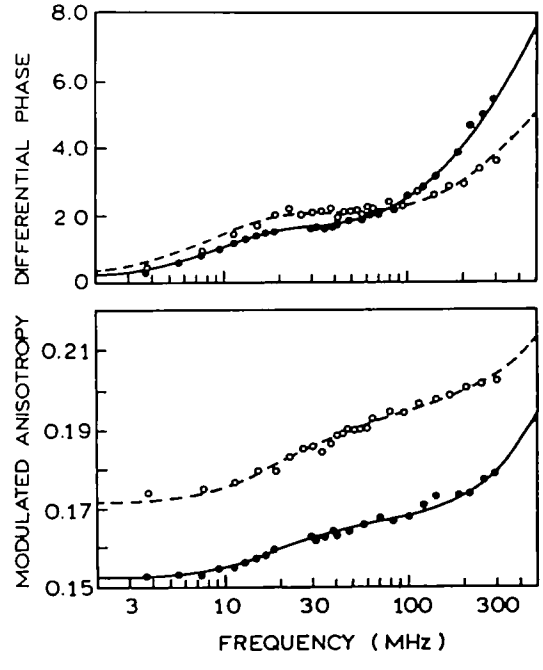


Fig. 7. **Anisotropy decays of S$\beta$gly in the absence (opened circles) and presence of 1-butanol (80 mM) (filled circles) at 30°C.** The differential phases and modulated anisotropies are shown in the upper and lower panels, respectively.

TABLE II. **Multi-exponential analysis of the intensity and anisotropy decays of S$\beta$gly fluorescence at 30°C in the absence and presence of 40 and 80 mM 1-butanol.**

| | Intensity decays | | | | | | Anisotropy decays | | | | | |
|---|---|---|---|---|---|---|---|---|---|---|---|---|
| | $\tau_1$ (ns) | $\tau_2$ (ns) | $\tau_3$ (ns) | $\alpha_1$ | $\alpha_2$ | $\alpha_3$ | $\chi^2$ | $\theta_1$ (ns) | $\theta_2$ (ns) | $r_0g_1$ | $r_0g_2$ | $\chi_2$ |
| S$\beta$gly | 0.73 | 3.14 | 8.22 | 0.319 | 0.468 | 0.213 | 0.9 | 0.17 | 39.8 | 0.088 | 0.19 | 0.9 |
| S$\beta$gly+40 mM 1-butanol | 1.46 | 2.43 | 8.05 | 0.102 | 0.540 | 0.358 | 1.1 | 0.20 | 53.1 | 0.101 | 0.175 | 0.9 |
| S$\beta$gly+80 mM 1-butanol | 1.98 | 2.34 | 7.72 | 0.125 | 0.534 | 0.341 | 1.1 | 0.19 | 58.0 | 0.120 | 0.161 | 0.9 |

particular, the center of the short component becomes longer, increasing from 0.54 to 2.2 ns, a value very close to that observed for monomeric tryptophan residues (*34*), while the width of the short component is reduced from 0.6 to 0.01 ns. The center of the long component increases to 7.5 ns and its width becomes sharp (from 5.9 to 0.33 ns). It is worth stating that the lifetime distribution analysis of Sβgly in the presence of 40 mM 1-butanol (data not shown) is consistent with the suggestion that the addition of alcohol to the protein solution results in a more flexible protein structure.

The frequency-domain anisotropy decays in the absence and presence of 40 and 80 mM 1-butanol are shown in Table II. The two-exponential anisotropy decays indicate both local motions of the tryptophanyl residues in Sβgly and an overall rotation of the macromolecule. The short correlation time in the range of 100–200 ps is associated with the local freedom of the tryptophanyl residues, as described in several anisotropy decay studies on proteins (*36, 37*). Correlation times longer than 40 ns are associated with the overall rotation of the protein. Figure 7 shows the anisotropy decays of Sβgly in the absence and presence of 80 mM 1-butanol. The differential phase data (upper panel in Fig. 7) show a decrease in the long correlation time amplitude at low frequencies near 20 MHz, and an increase in the short correlation time amplitude at higher frequencies near 20 MHz. The observed changes in the anisotropy decays induced by the addition of 1-butanol suggest that the alcohol induces additional freedom in the tryptophanyl residues and that in turn confers more flexibility to the protein.

*Conclusions*—Understanding protein behavior in biological reactions is fundamental for shedding light on the mechanism(s) governing biochemical processes and determining the influence of the polypeptide chain on the active site. The biological activity and native structure of a protein are strictly linked: small structural alterations in the macromolecule may have profound effects on protein behavior. It is well known that solvent composition affects both the structural and functional properties of biological macromolecules; multi-component solvents such as aqua-alcohol mixtures have been shown to have a significant influence on the thermodynamic stability of a number of proteins (*38*). Our data show that Sβgly is a very stable protein; in fact it is active at high temperature and in the presence of organic solvents. The presence of different alcohols causes a marked enzyme activation at low temperature that is dependent on the concentration and alkyl chain length of the alcohol. The CD and FT-IR analyses point out that the secondary structure of the protein is not affected at low temperatures by the presence of 1-butanol. The fluorescence and anisotropy decay data suggest that the addition of 80 mM 1-butanol to the protein solution produces some effect on the protein microenvironment, inducing a more flexible protein structure that is probably the cause of the increased enzyme activity. Moreover, in this paper, we also show the power of time-resolved fluorescence to detect small environmental changes in the protein structure not observed by other techniques. The fluorescence data indicate that 1-butanol and other alcohols at the concentrations that result in maximal activation, induce more flexibility in the protein allowing a higher catalytic activity.

We thank Mr. Carlo Vaccaro and Mr. Ottavio Piedimonte for their technical assistance and Prof. Paolo Bazzicalupo for useful discussion. We also thank Dr. Z. Gryczynski for his assistance with the fluorescence measurements.

## REFERENCES

1. Jaenicke, R., Schuring, H., Beaucamp, N., and Ostendorp, R. (1996) Structure and stability of hyperstable proteins: glycolitic enzymes from hyperthermophilic bacterium *Thermotoga maritima*. *Adv. Protein Chem.* **48**, 181–269
2. Sthal, S. (1993) Thermophilic microorganisms: the biological background for thermophily and thermoresistance of enzymes in *Thermostability of Enzymes* (Gupta, M.N., ed.) pp. 45–74, Springer-Verlag, Berlin
3. Shoichet, B.K., Baase, W.A., Kurozi, R., and Matthews, W. (1995) A relationship between protein stability and protein function. *Proc. Natl. Acad. Sci. USA* **92**, 452–456
4. Vihinem, M. (1987) Relationship of protein thermostability. *Protein Eng.* **1**, 477–480
5. Martinek, K. and Mozhaev, V.V. (1993) Need for thermostability, its benefits and main strategies for thermostabilization in *Thermostability of Enzymes* (Gupta, M.N., ed.) pp. 76–82, Springer-Verlag, Berlin
6. Mozhaev, V.V. and Martinek, K. (1990) Thermostable enzymes: Current and future applications in biotechnology. *Adv. Drug. Deliv. Rev.* **4**, 387–393
7. De Rosa, M., Gambacorta, A., and Bu' Lock, J.D. (1975) Extremely thermophilic acidophilic bacteria convergent with *Sulfolobus solfataricus*. *J. Gen. Microbiol.* **86**, 156–164
8. Pisani, F.M., Rella, R., Rozzo, C., Raia, C.A., Nucci, R., Gambacorta, A., De Rosa, M., and Rossi, M. (1990) Thermostable β-galactosidase from the archaebacterium *Sulfolobus solfataricus*. Purification and properties. *Eur. J. Biochem.* **187**, 321–328
9. Nucci, R., Moracci, M., Vaccaro, C., Vespa, N., and Rossi, M. (1993) Exo-glucosidase activity and substrate specificity of the β-glycosidase from the extreme thermophilic *Sulfolobus solfataricus*. *Biotechnol. Appl. Biochem.* **17**, 239–250
10. Cubellis, M.V., Rozzo, C., Montecucchi, P., and Rossi, M. (1990) Isolation and sequencing of a new β-galactosidase-encoding archaebacterial gene. *Gene* **94**, 89–94
11. Moracci, M., La Volpe, A., Pulitzer, J.F., Rossi, M., and Ciaramella, M. (1992) Expression of the thermostable β-galactosidase gene from the archaebacterium *Sulfolobus solfataricus* in *Saccharomyces cerevisiae* and characterization of a new inducible promoter for heterologous expression. *J. Bacteriol.* **174**, 873–882
12. Moracci, M., Nucci, R., Febbraio, F., Vaccaro, C., Vespa, N., La Cara, F., and Rossi, M. (1995) Expression and extensive characterization of the β-glycosidase from the extreme thermoacidiphilic archaeon *Sulfolobus solfataricus* in *E. coli*. Authenticity of the recombinant enzyme. *Enzyme Microb. Technol.* **17**, 992–997
13. D'Auria, S., Morana, A., Febbraio, F., Vaccaro, C., De Rosa, M., and Nucci, R. (1996) Functional and structural properties of the homogenous β-glycosidase from the thermoacidophilic archaeon *Sulfolobus solfataricus* expressed in *Saccharomyces cerevisiae*. *Protein Expression Purif.* **7**, 299–308
14. Pearl, L.H., Hemmings, A.M., Nucci, R., and Rossi, M. (1993) Crystallization and prelyminary X-ray diffraction of the β-glycosidase from the thermophilic archaeon *Sulfolobus solfataricus*. *J. Mol. Biol.* **229**, 561–563
15. Aguilar, C.F., Sanderson, I., Moracci, M., Ciaramella, M., Nucci, R., Rossi, M., and Pearl, L.H. (1997) Crystal structure of the β-glycosidase from the hyperthermophilic archaeon *Sulfolobus solfataricus*: resilience as a key factor in thermostability. *J. Mol. Biol.* **271**, 789–802
16. Barlow, D.J. and Thornton, J.M. (1983) Ion-pairs in proteins. *J. Mol. Biol.* **168**, 857–885
17. Nucci, R., D'Auria, S., Febbraio, F., Vaccaro, C., Morana, A., De Rosa, M., and Rossi, M. (1995) A thermostable β-glycosidase from *Sulfolobus solfataricus*: Temperature and SDS effects on its functional and structural properties. *Biotechnol. Appl. Biochem.* **21**, 265–274

18. D'Auria, S., Rossi, M., Barone, G., Catanzano, F., Del Vecchio, P., Graziano, G., and Nucci, R. (1996) Temperature induced denaturation of a β-glycosidase from the archaebacterium *Sulfolobus solfataricus*. *J. Biochem.* **120**, 292-300
19. D'Auria, S., Rossi, M., Nucci, R., Irace, G., and Bismuto, E. (1997) Perturbation of conformational dynamics, enzymatic activity and thermostability of β-glycosidase from archaeon *Sulfolobus solfataricus* by pH and sodium dodecyl sulfate detergent. *Proteins Struct. Funct. Genet.* **27**, 71-79
20. D'Auria, S., Barone, R., Rossi, M., Nucci, R., Barone, G., Fessas, D., Bertoli, E., and Tanfani, F. (1997) Effects of temperature and SDS on the structure of β-glycosidase from the thermophilic archaeon *Sulfolobus solfataricus*. *Biochem. J.* **323**, 833-840
21. Bismuto, E., Irace, G., D'Auria, S., Rossi, M., and Nucci, R. (1997). Multitryptophan-fluorescence-emission decay of β-glycosidase from the extremely thermophilic archaeon *Sulfolobus solfataricus*. *Eur. J. Biochem.* **244**, 53-58
22. Catanzano, F., Graziano, G., De Paola, B., Barone, G., D'Auria, S., Rossi, M., and Nucci, R. (1998) Guanidine-induced denaturation of β-glycosidase from the archaeon *Sulfolobus solfataricus* expressed in *Escherichia coli*. *Biochemistry* **37**, 14484-14490
23. D'Auria, S., Moracci, M., Febbraio, F., Tanfani, F., Nucci, R., and Rossi, M. (1998) Structure-function studies on β-glycosidase from *Sulfolobus solfataricus*. Molecular bases of thermostability. *Biochimie* **80**, 949-957
24. Bradford, M.M. (1976) A rapid and sensitive method for the quatification of microgram quantities of protein utilizing the principle of protein-dye binding. *Anal. Biochem.* **72**, 248-254
25. Lakowicz, J.R., Laczko, G., and Gryczynski, I. (1986) A 2 GHz frequency-domain fluorometer. *Rev. Sci. Instrum.* **57**, 2499-2504
26. Lakowicz, J.R., Laczko, G., Gryczynski, I., and Cherek, H. (1986) Measurement of subnanosecond anisotropy decays of protein fluorescence using frequency-domain fluorometry. *J. Biol. Chem.* **261**, 2240-2248
27. Laczko, G., Gryczynski, I., Gryczynski, Z., Wiczk, W., Malak, H., and Lakowicz, J.R. (1990) A 10 GHz frequency domain fluorometer. *Rev. Sci. Instrum.* **61**, 92331-9237
28. Lakowicz, J.R., Laczko, G., Cherek, H., Gratton, E., and Limkeman, H. (1984) Analysis of fluorescence decay kinetics from variable-frequency phase shifts and modulation data. *Biophys. J.* **46**, 463-477
29. Lakowicz, J.R., Cherek, H., Maliwal, B., and Gratton, E. (1985) Time-resolved fluorescence anisotropies of fluorophores in solvents and lipid bilayers obtained from frequency-domain phase-modulation fluorometry. *Biochemistry* **24**, 376-383
30. Strickland, E.H. (1974) Aromatic contributions to circular dichroism spectra of proteins CRC. *Crit. Rev. Biochem.* **2**, 113-175
31. Chirgadze, Y.N., Fedorow, O.W., and Trushina, N.P. (1975) Estimation of amino acid residue side-chain absorption in the infrared spectra of protein solutions in heavy water. *Biopolimers* **14**, 679-694
32. Fernandez-Ballester, G., Castresana, J., Arrondo, J.R.L., Ferragut, J.A., and Gonzales-Ros, J.M. (1992) Protein stability and interaction of the nicotinic acetylcholine receptor with cholinergic ligands studied by Fourier-transform infrared spectroscopy. *Biochem. J.* **288**, 421-426
33. Banecki, B., Zylicz, M., Bertoli, E., and Tanfani, F. (1992) Structural and functional relationships in DnaK and DnaK756 heat-shock proteins from *Escherichia coli*. *J. Biol. Chem.* **267**, 25051-25058
34. Lakowicz, J.R. (1986) *Principles of Fluorescence Spectroscopy*, Plenum Press, New York
35. Lakowicz, J.R., Cherek, H., Gryczynski, I., Joshi, N., and Jonhson, L.M. (1987) Analysis of fluorescence decay kinetics measured in frequency-domain using distribution of decay times. *Biophys. Chem.* **28**, 35-50
36. Lakowicz, J.R., Gryczynski, I., Cherek, H., and Laczko, G. (1991) Anisotropy decays of indole, melittin monomer and melittin tetramer by frequency-domain fluorometry and multi-wavelength global analysis. *Biophys. Chem.* **39**, 241-251
37. Lakowicz, J.R., Gryczynski, I., Szmacinski, H., Cherek, H., and Joshi, N. (1991) Anisotropy decays of single tryptophan proteins measured by GHz frequency-domain fluorometry with collisional quenching. *Eur. Biophys. J.* **19**, 125-140
38. Dill, A. (1990) Dominant forces in protein folding. *Biochemistry* **29**, 7133-7155